engineering proceedings

MDPI

Proceeding Paper

Experimental Characterization of a Compact Gyroid-Pipe Heat Exchanger for Fuel Cell Powered Electric Aircraft Propulsion †

Chetan Kumar Sain *, Jeffrey Haensel, Sebastian Merbold, Franz-Theo Schoen and Stefan Kazula

Institute of Electrified Aero Engines, German Aerospace Centre (DLR), 03046 Cottbus, Germany; jeffrey.haensel@outlook.de (J.H.); sebastian.merbold@dlr.de (S.M.); franz-theo.schoen@dlr.de (F.-T.S.); stefan.kazula@dlr.de (S.K.)

* Correspondence: chetan.sain@dlr.de

† Presented at the 15th EASN International Conference, Madrid, Spain, 14–17 October 2025.

Abstract

The future of low-emission aviation lies in electric aircraft propulsion systems based on fuel cells. One of the challenge lies in designing and testing critical components, such as heat exchangers, and studying their impact on system-level performance and power densities. This paper presents the design and experimental characterization of a compact TPMS gyroid-pipe heat exchanger with embedded coolant channels. Thermal–hydraulic performance is quantified using heat transfer rates and pressure drop measurements. Three design variants of the gyroid pipe are prototyped and experiments are performed for a range of mass flow rates and temperatures. The results are presented in terms of heat exchanger characteristics and the design operating points are determined. A comparison is made between the gyroid-pipe design and a conventional louvered-fin-plate heat exchanger. The results show that the louvered-fin-plate design outperforms the gyroid-pipe design, mainly due to higher pressure loss. Additional design variants of the gyroid-pipe heat exchanger, in which the TPMS curvatures are stretched along the air length, improve the thermal and hydraulic performance. The gyroid-pipe heat exchanger design is beneficial as its volumetric and gravimetric power densities are higher than those of a conventional heat exchanger. This is important for reducing the mass of the system and ensuring the feasibility of a fuel cell system in aviation.

Keywords: thermal management; compact heat exchanger; thermal–hydraulic performance; TPMS gyroid heat exchanger; heat exchanger characteristics; heat exchanger sizing

1. Introduction

An all-electric aircraft powered by a low-temperature polymer electrolyte membrane fuel cell system (LTPEMFCS) has the potential to achieve the strategic aim of low-emission flights by 2050 [1]. However, regional flights with 70 passengers are not yet feasible with current technologies due to the low mass-specific power densities of its components. This is particularly true for the large components, such as the heat exchanger (HEX), which is essential to the thermal management system (TMS) and must be lighter, more compact and more efficient than the current state of the art. The roadmap for PEM-based propulsion technology estimates a specific heat rejection of 10 kW/kg and a tolerable 20% power loss by the year 2026 for LTPEMFCS cooling [2]. HEXs, based on triple periodic minimal surface (TPMS) structures, are getting into focus as they offer high compactness and smooth continuous curvatures [3]. This paper introduces a HEX design that uses the

Academic Editors: Spiros Pantelakis, Andreas Strohmayer and Gustavo Alonso

Published: 24 April 2026

TPMS gyroid unit cell with embedded channels for liquid coolant and is denoted as the gyroid-pipe (GyP) HEX. This study aims to quantify the thermal–hydraulic performance of the GyP HEX with its three design variants and to compare it with that of a conventional louvered-fin-plate (LFP) compact HEX. Small-scale GyP HEX prototypes, along with a thermal management test modular air duct (TMTMAD) setup for experimental testing, are developed and described. Furthermore, methodology for the data acquisition and processing for the characterization of the HEX performance is explained. The HEX rating results are presented in terms of the measured heat transfer rate and pumping power as a function of pressure drop. The ratio of heat transfer rate to the pumping power is defined as the power ratio (PR). The maximum performance point is selected for a PR of >5, for the targeted 20% loss according to the roadmap [2], depicting an output heat duty that is five times higher than the input pumping power. The comparative results between the design variants of GyP and LFP HEXs are summarized.

2. Design of GyP HEX

Of the various TPMS geometries, the gyroid offers the smoothest zero mean curvature, enabling high convective heat transfer by mixing the hot near-wall flow with the colder core flow [3]. Gyroid sheets offer design variations using surface grading, which can be utilized to optimize the channels for low pressure gradients, especially for the air flow with high Reynolds numbers [4]. Compared with the commonly used plate-fin HEX, gyroid has higher stiffness and a smaller stress signature due to the 3D distribution of its lattice structure and lack of sharp corners [5]. The potential of gyroid is utilized in the GyP HEX design due to its thermal–hydraulic and structural properties relative to other types of TPMS geometries. This work involves a GyP with embedded coolant channels in an air–liquid cross-flow configuration, which is described briefly in the following section and in Figure 1. A detailed design description of GyP HEX can be found in reference [6].

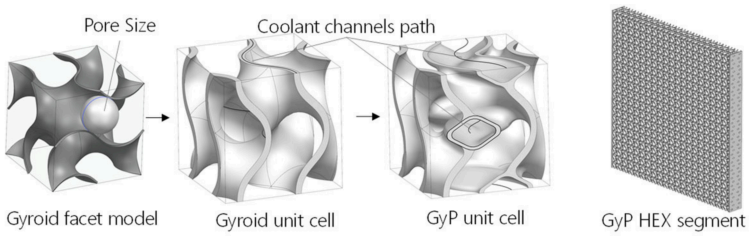

Figure 1. TPMS GyP unit cell design development sequence (left to right) and mockup of HEX core segment using 800 GyP unit cells (right).

The unit cell for GyP HEX is designed using gyroid's implicit equation and surface modeling. The facet model is then converted into a thin-wall solid model with a constant wall thickness of 0.5 mm. Additional coolant channels are designed, embedded into the gyroid wall curvatures. They follow the splines derived at the mid-surface of these walls, as indicated in Figure 2, bottom. An oval cross-section is selected for the coolant channels because of its aerodynamic shape and tolerable angles for additive manufacturing, as shown in the GyP unit cell in Figure 2, bottom. A total of 800 GyP unit cells are arranged sequentially inside a 200 mm × 200 mm × 20 mm volume to generate the GyP HEX core. This design results in 39 pairs of coolant channels arranged in a cross-flow configuration along its height as shown in Figure 2. Additionally, two variants with thicknesses of 30 mm and 40 mm are created by stretching the unit cells along its air length. Prototypes are developed using additive manufacturing and these designs are denoted as GyP-20, GyP-30, and GyP-40 with their respective thicknesses of 20, 30, and 40 mm. Table 1 lists the key design attributes for each GyP variant and for the LFP.

https://doi.org/10.3390/engproc2026133078

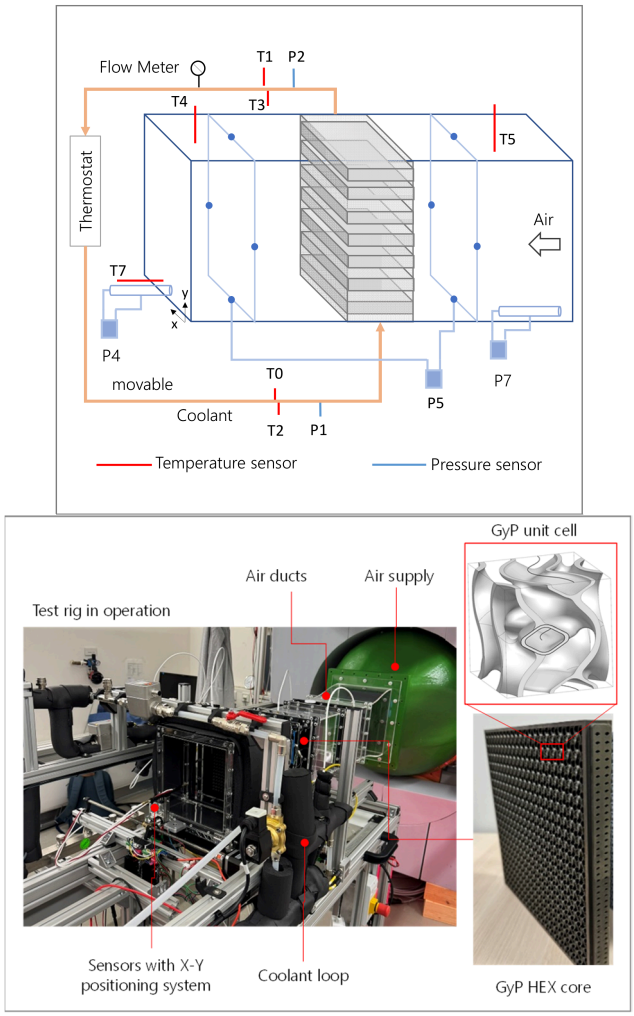

Figure 2. Schematic of TMTMAD (**top**); HEX prototype and experimental setup (**bottom**).

Table 1. Key design attributes for gyroid-pipe and louvered-fin-plate HEXs.

Design	Unit	GyP-20	GyP-30	GyP-40	LFP
Thickness	mm	20	30	40	62
Frontal area	mm	200 × 200	200 × 200	200 × 200	180 × 180
Mass	kg	1.1	1.65	2.2	3.9
Air wetted area	m^2	0.50	0.69	0.89	1.51
Air volume	10^{-3} m^3	0.49	0.75	0.99	1.24
Compactness	m^2/m^3	1012	930	896	1222

The LFP HEX is a compact design and belongs to an oil cooling application. It has an air-side frontal cross-section of 180 mm × 180 mm and a thickness of 62 mm. This LFP offers 20.7% higher compactness on the air side and has additional fins inside the coolant plates to enhance turbulence and heat transfer. Its choice was made due to its compact design and comparable test domain.

3. Experimental Study

The thermal–hydraulic characteristics of the HEX are experimentally determined using TMTMAD connected to an external wind tunnel facility. The experimental setup consists of a test section with HEX, connected to cold air and hot coolant loops, as illustrated by the simplified schematic in Figure 2, top.

The air loop contains an air supply, which is connected externally to the aero-acoustic wind tunnel of Brandenburg University of Technology, Cottbus-Senftenberg, located in the Fluid Centrum laboratory. The wind tunnel outlet is redirected into a 200 mm × 200 mm square, modular duct. Within this duct the HEX is positioned in between symmetrically arranged pressure and temperature measurement points. Dynamic pressure is measured by the Pitot tubes P_7 and P_4. To measure varying temperature and velocity fields behind the HEX, a PT100 probe T_4 (TMH Temperatur Messelemente Hettstedt GmbH, Maintal, Germany) and Prandtl tube P_4 are placed on an X-Y positioning system, as shown in Figure 2, top. Sensor P_5 measures the differential pressure before and after the HEX. The pressure range is 7.5 kPa, monodirectional with an accuracy of ±0.01875 kPa. The coolant loop is connected to a HUBER CC 510 Temperature control (Peter Huber Kaeltemaschinenbau SE, Offenburg, Germany) unit, which controls the volume flow up to 5 L/min and bath temperature up to 80 °C, using water as a coolant. A maximum rejected heat of 6.2 kW is measured on the coolant side. Coolant temperature at the HEX inlet and outlet are measured using multiple sensors, T_0, T_1, T_2, and T_3, and the temperature difference is calculated using an average of the cross values, $(T_0 - T_1)$ and $(T_2 - T_3)$. Pressure loss inside the coolant loop across the HEX is measured with a differential pressure sensor attached between P_2 and P_1 as shown in Figure 2, top. The control and data acquisition is programmed in Labview (Version 2024 Q1, National Instrument Emerson, Austin, TX, USA, 2024), using a CompactRIO controller from National Instruments (National Instrument Emerson, Austin, TX, USA, 2024). Tests are performed at coolant HEX inlet temperatures of 60 °C, 70 °C, and 80 °C, with coolant flow rates of 1, 3, and 5 L/min, and each for air speeds of up to 30 m/s. The next section explains the data processing and results used to characterize the thermal–hydraulic performance of the aforementioned HEXs.

4. Data Processing and Results

The performance of a HEX can be measured by its combined thermal and hydraulic characteristics. The HEX rating describes thermal and hydraulic performance. Thermal performance is quantified by the heat transfer rate $\dot{Q} = \dot{m} \cdot C_P \cdot (T_{in} - T_{out})$, defined as a product of the mass flow rate $\dot{m}$, the specific heat capacity C_P, and the temperature difference between the HEX inlet and outlet. The mass flow rate $\dot{m}$ is calculated as the product of density ρ, velocity C, and cross-sectional area A as $\dot{m} = \rho \cdot C \cdot A$. The densities of air and water are taken as constants, $\rho_{air} = 1.176\ kg/m^3$ and $\rho_{water} = 988.05\ kg/m^3$, respectively. The air velocity is calculated as $C_{air} = \sqrt{2 \cdot P_7 / \rho_{air}}$, using the dynamic pressure P_7. The cross-section is taken as a constant of A = 0.2 m × 0.2 m, and the mass flow rate at the coolant loop is measured using a flow meter. The specific heat capacities are taken as $C_{P,air} = 1006\ J/kg\ K$ and $C_{P,air} = 4030\ J/kg\ K$. The temperature difference $(T_7 - T_5)$ across the HEX, along the air side, is calculated using the calibrated values. The location of T_7 is determined near the average value location after the grid resolution measurements, performed at the HEX outlet using the X-Y positioning system. Compared with measurements taken with T7 using the X-Y positioning system on GyP HEX, T4 at a fixed position resulted in uncertainty of 0.48%, underpredicting the outlet temperature. A similar observation was made with LFP but with a much higher deviation of 2.5%. This position changes for some multifactorial reasons, which in the end make the air side outlet temperature measurement less trustworthy for calculating the heat transfer rate than the liquid side measurement.

The hydraulic performance of a HEX can be quantified by the Pumping Power PP, required by the air blower and the coolant pump to overcome the pressure losses inside the HEX. This is the product of the volume flow rate $\dot{V}$ and the pressure drop ΔP_{loss} across the HEX, divided by the compressor efficiency η as $PP = \dot{V} \cdot \Delta P_{loss} / \eta$. In this study, efficiency

is set to one and the volume flow rate is calculated as the product of density and the mass flow rate as $\dot{V} = \dot{m} \cdot \rho$. The pressure drop ΔP_{loss} is measured using the P_5 differential pressure sensor across the air side and the pressure difference between P_1 and P_2 across the coolant side.

The combined thermal–hydraulic performance of a HEX is determined by the power ratio, which is the heat transfer rate divided by the pumping power as $PR = PP/\dot{Q}$. This ratio shows the increase in heat rejection from the HEX for each unit of input pumping power. Higher power ratios are ideal for economic and system-level gravimetric power densities of HEXs. This study aims for power ratios of five or higher, indicating that the HEX should deliver a heat transfer rate that is five times higher than the consumed pumping power [2].

Before full thermodynamical testing, the parametrization of the GyP structure was investigated by pure aerodynamical testing, using GyP-20, GyP-30, and GyP-40, the results of which can be found in reference [6]. In this study, the GyP-20 structure was chosen to perform a full thermodynamical test, for which it was manufactured in Inconel 718 alloy, by using a selective laser melting technique.

The heat transfer rate can be calculated on the air and water sides across the HEX. In an ideal isothermal system, these values are equal. The surfaces of the HEX that are exposed, as well as the air ducts and coolant lines adjacent to the HEX, are insulated with the appropriate type and amount of insulation tape and thermal blankets. Despite these measures, differences in heat transfer rates between the air and water sides are observed, as shown in Figure 3 on the left.

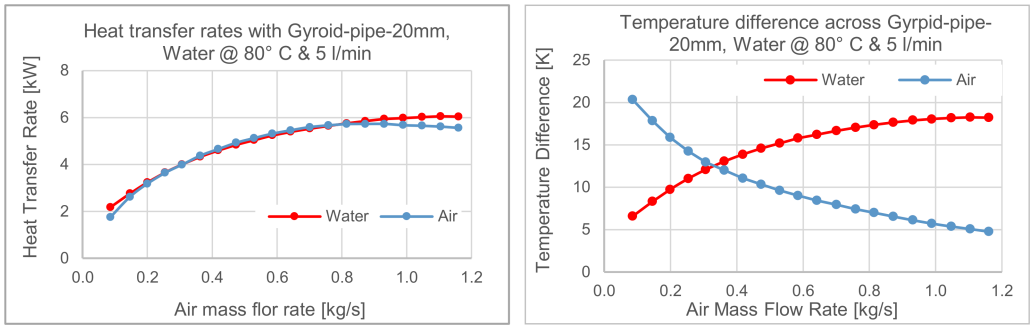

Figure 3. Comparison of heat transfer rates in air and coolant loop (**left**), temperature differences in air and coolant loop (**right**) across the gyroid-pipe HEX with 20 mm thickness.

The mismatch in the heat transfer rates occurs mainly due to temperature measurements at a fixed location in the air outlet cross-section. As mentioned before, a movable rig of pressure P_7 and temperature T_7 sensors is used to determine their mean values and locations across the air outlet cross-section. To measure the full pressure and velocity fields would be too time-consuming, which limits the operation of the air supply unit.

Additionally, Figure 3, right, depicts the temperature differences in the air and water loops across the GyP-20. It shows that the temperature difference across the hot water side increases and the temperature difference across the cool air side decreases with higher air mass flow rates. This represents heat transfer from the hot coolant side to the cold air side. In a typical LTPEMFCS, a maximum temperature difference of 15 K is required in the coolant loop to maintain the system's operating temperature. The GyP-20 HEX fulfils this requirement with an air mass flow rate of $\dot{m}_{air} = 0.5$ kg/s, as plotted in Figure 3 under the titled boundary conditions. A temperature difference of up to 18.2 K at the water side can be achieved with higher air mass flow rates. This means that a portion of the coolant can be overcooled inside the HEX and mixed with the rest of the bypassed hot coolant before reentering the LTPEM fuel cell system with the required inlet temperature. Operating

points with overcooled coolant (with a temperature difference above 15 K) can be selected for specific air mass flow rates in the heat transfer characteristics plots.

Figure 4 shows the HEX characteristics as plots of the heat transfer rate $\dot{Q}$ and pumping power PP in kW on the primary axis and the power ratio PR on the secondary axis, plotted against the air mass flow rate, $\dot{m}_{air}$. The heat transfer rate increases with air mass flow. LFP shows greater heat duty than GyP-20 for similar air flow rates as the LFP_$\dot{Q}$ is higher than GyP-20_$\dot{Q}$. For relevant range from $\dot{m}_{air}$ = 0.4 kg/s to 0.6 kg/s, it has a heat transfer rate that is around 16% higher than GyP-20, as mentioned in Figure 4.

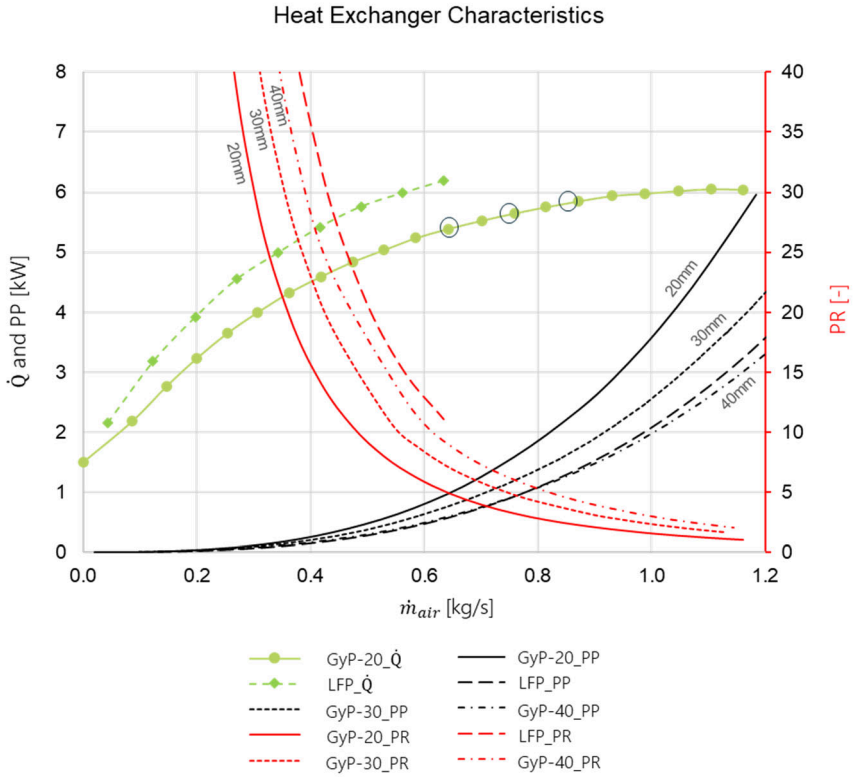

Figure 4. Heat exchanger characteristics in terms of heat transfer rate, pumping power and power ratio over the air mass flow rate for gyroid-pipe and louvered-fin-plate HEXs.

As seen in Table 1, LFP offers higher compactness and air volume than GyP-20, which could lead to a potential heat transfer surface that is three times higher than GyP-20.

The pumping power increases as the pressure drops due to viscous and form drag increases. The highest pressure drop is measured with the GyP-20 at a specific air mass flow rate. Designs with larger air side thickness, such as GyP-30 and GyP-40, have reduced the pumping power by −11% and −25% respectively at an air mass flow rate of 0.65 kg/s relative to GyP-20. The GyP-40 design shows slightly better hydraulic performance than the LFP design, as the pumping power values lie lower as plotted in Figure 4. Combined performance is assessed in terms of the power ratio, which drops dramatically as the pumping power increases. The operating point for the HEX can be selected based on the heat transfer rate and air mass flow rate at which the power ratio of five is achieved. This represents an economical design point for the HEX, delivering a heat duty five times higher than the input pumping power. The operating point for the LFP results in the highest possible heat transfer rate of 6.2 kW and a power ratio of 11, at an air mass flow rate of 0.63 kg/s, equivalent to an air speed of 13.5 m/s. As shown in Table 2, the LFP results in a pumping power of 0.56 kW and a gravimetric power density of 1.59 kW/kg. Comparing LFP with GyP-10, LFP delivers 15.9% higher heat duty at 47.6% less pumping power and

at a similar air mass flow rate. As drawback of LFP size, it results in 54% less volumetric power density and 67% less gravimetric power density than GyP-10.

Table 2. Key results for HEX rating with gyroid-pipe and louvered-fin-plate HEXs.

HEX Rating	Unit	GyP-20	GyP-30	GyP-40	LFP
Heat transfer	kW	5.35	5.68	5.75	6.2
Pumping power	kW	1.07	1.12	1.13	0.56
Air mass flow rate	kg/s	0.63	0.75	0.82	0.63
Air inlet velocity	m/s	13.6	15.7	17.4	13.5
Volumetric power density	kW/m^3	10,769	7622	5787	5009
Gravimetric power density	kW/kg	4.86	3.44	2.61	1.59

Figure 4 shows the operating points of all three variants of GyP HEX. At their respective power ratios of five, the GyP-20, GyP-30, and GyP-40 result in heat transfer rates of 5.35 kW, 5.68 kW, and 5.75 kW, respectively. As the GyP thickness increases, the pumping power curves sink and a power ratio of five is achieved at higher heat transfer rates. However, this gain comes at a price of higher pumping power, as listed in Table 2. As the thickness increases from 20 mm to 30 and 40 mm, the size and mass of the GyP HEX increase. Consequently, the volumetric and gravimetric power densities decrease relative to GyP-20. However, the LFP outperforms the GyP in terms of high heat transfer and low pumping power; GyP results in general higher volumetric and gravimetric power densities than LFP due to its smaller thickness and choice of material. Using the rating results of GyP and LFP, which are measured using small-scale prototypes, an estimation of full-scale HEX size for the LTPEMFCS cooling requirements can be realized in future work.

5. Conclusions and Outlook

This work presents the design and experimental characterization of a TPMS-based GyP HEX. It illustrates the design of the GyP HEX and the test rig. The data reveals the thermal–hydraulic performance of the HEX, characterized by the heat transfer rate and pumping power. Performance points for the HEX were selected to achieve a minimum power ratio of five, ensuring economical operation. However, the conventional LFP outperforms the TPMS GyP in terms of total heat duty and pumping power; the GyP achieves a higher gravimetric power density, which would reduce the total mass of the TMS at system level. Additionally, the GyP HEX's higher volumetric power density relative to the LFP is beneficial for HEX integration inside the propulsion system, as the required volume for a full-scale TMS would be reduced without compromising thermal performance. Increasing the thickness along the air side with GyP-30 and GyP-40 results in smoother TPMS curvatures than with GyP-20, reducing the pressure drop and consequent pumping power. This demonstrates the potential for further performance improvements relative to conventional plate-fin compact HEXs. Future work will involve conducting a design of experiment to determine the optimum set of design parameters for the TPMS GyP HEX. Optimization on the GyP design is needed as the target values of specific heat transfer rates of 10 kW/kg are not achieved. Additionally, work will be conducted using the test data of small-scale prototypes, to estimate the full-scale HEX size for the TMS of an LTPEMFCS as per the system requirements.

Author Contributions: Conceptualization, C.K.S.; methodology, C.K.S., J.H., S.M. and F.-T.S.; software, J.H.; validation, J.H., C.K.S. and F.-T.S.; formal analysis, C.K.S., F.-T.S., J.H. and S.M.; investigation, C.K.S. and F.-T.S.; resources, S.K.; writing—original draft preparation, C.K.S. and F.-T.S.; writing—review and editing, all; visualization, C.K.S.; supervision, S.M., F.-T.S. and S.K.; project

administration, C.K.S., J.H. and S.K.; funding acquisition, S.K. All authors have read and agreed to the published version of the manuscript.

Funding: This research received no external funding.

Institutional Review Board Statement: Not applicable.

Informed Consent Statement: Not applicable.

Data Availability Statement: No new data is available.

Acknowledgments: We would like to acknowledge Thomas Geyer and Christoph Egbers of the Brandenburg University of Technology Cottbus-Senftenberg for the use of the aero-acoustic wind tunnel.

Conflicts of Interest: The authors declare no conflict of interest.

Abbreviations

The following abbreviations are used in this manuscript:

TPMS	Triple Periodic Minimal Surface
LTPEMFCS	Low-Temperature Polymer Electrolyte Membrane Fuel Cell System
HEX	Heat Exchanger
TMS	Thermal Management System
GyP	Gyroid Pipe
LFP	Louver-Fin-Plate
TMTMAD	Thermal Management Test Modular Air Duct
PP	Pumping Power
PR	Power Ratio

References

1. Air Transport Action Group. Waypoint2050. September 2020. Available online: https://www.atag.org (accessed on 1 February 2026).
2. Webber, H.; Llambrich, J.; Davoudi, H. Thermal Management Roadmap Report. Available online: https://www.ati.org.uk/wp-content/uploads/2022/03/FZO-PPN-COM-0019-Thermal-Management-Roadmap-Report.pdf (accessed on 1 February 2026).
3. Li, N.; Wang, M.; Zhao, J.; Sun, K.; Bi, C.; Du, M.; You, E.; Yang, M. Heat Transfer Characterization of TPMS Heat Exchangers Applied to the Aerospace Field. *Front. Heat Mass Transf.* **2025**, *23*, 601–614. [CrossRef]
4. Al-Ketan, O.; Ali, M.; Khalil, M.; Rowshan, R.; Khan, K.A.; Abu Al-Rub, R.K. Forced Convection Computational Fluid Dynamics Analysis of Architected and Three-Dimensional Printable Heat Sinks Based on Triply Periodic Minimal Surfaces. *J. Therm. Sci. Eng. Appl.* **2021**, *13*, 021010. [CrossRef]
5. Yu, X.; Moreira, T.A.; Chen, B.; Rankouhi, B.; Thoma, D.J.; Anderson, M.H.; Qian, X. Data-driven optimization, additive manufacturing and thermohydraulic testing of a high-temperature Gyroid-based TPMS heat exchanger. *Appl. Therm. Eng.* **2025**, *280*, 128422. [CrossRef]
6. Sain, C.K.; Mathiazhagan, A.; Bhapkar, S.; Kazula, S.; Asli, M.; Höschler, K. Design Assessment and Test of Compact Gyroid-TPMS Heat Exchanger with Embedded Coolant Channels for LTPEM Fuel Cell Powered Regional Aircraft. In Proceedings of the DLRK 2025, Augsburg, Germany, 23–25 September 2025.